
Article:
Colebatch, Annie L., McKay, Alasdair I., Beattie, Nicholas A. et al. (2 more authors) (2017) Fluoroarene Complexes with Small Bite Angle Bisphosphines:Routes to Amine–Borane and Aminoborylene Complexes. EUROPEAN JOURNAL OF INORGANIC CHEMISTRY. pp. 4533-4540. ISSN 1434-1948

https://doi.org/10.1002/ejic.201700600

ChemPubSoc Europe

DOI: 10.1002/ejic.201700600

EurJIC European Journal of Inorganic Chemistry

Full Paper

Aminoborylene Complexes

CLUSTER ISSUE

Fluoroarene Complexes with Small Bite Angle Bisphosphines: Routes to Amine–Borane and Aminoborylene Complexes

Annie L. Colebatch,[a] Alasdair I. McKay,[a] Nicholas A. Beattie,[b] Stuart A. Macgregor,*[b] and Andrew S. Weller*[a]

Abstract: Fluoroarene complexes of the small bite angle bisphosphine $Cy_2PCH_2PCy_2$ (dcpm) have been prepared: [Rh(dcpm)(η^6-1,2-$F_2C_6H_4$)][Al{OC(CF_3)$_3$}$_4$] and [Rh(dcpm)(η^6-1,2,3-$F_3C_6H_3$)][Al{OC(CF_3)$_3$}$_4$]. These complexes act as precursors to a previously inaccessible σ-amine–borane complex [Rh(dcpm)(η^2-H_3B•NMe_3)][Al{OC(CF_3)$_3$}$_4$] of a small bite-angle phosphine. This complex is a poor catalyst for the dehydrocoupling of H_3B•NMe_2H. Instead, formation of the bridging borylene complex [{RhH(μ-dcpm)}$_2$(μ-H)(μ-$BNMe_2$)][Al{OC(CF_3)$_3$}$_4$] occurs, which has been studied by NMR, mass spectrometry, crystallographic and DFT techniques. This represents a new route to bridging borylene complexes.

Introduction

The transition metal catalysed dehydrocoupling and dehydropolymerisation of amine–boranes has been the subject of considerable recent attention due to both fundamental interest in BH/NH activation processes and as routes to new BN-based materials.[1–3] Amine–borane σ-complexes[4] are often implicated as intermediates in such processes. Although a wide variety of amine–borane σ-complexes are now known,[4–6] previous attempts to prepare such species with small bite angle bisphosphine coligands have been unsuccessful.[7] Studying the reactivity of [Rh{$Ph_2P(CH_2)_xPPh_2$}(η^6-FC_6H_5)][BAr^F_4] with H_3B•NMe_3 to form [Rh{$Ph_2P(CH_2)_xPPh_2$}(η^2-H_3B•NMe_3)][BAr^F_4] [x = 2–5, Ar = 3,5-$(CF_3)_2C_6H_3$] revealed a dependence of the relative strengths of the metal-borane/metal–arene interactions on the P–Rh–P bite angle (Scheme 1a).[8,9] Larger bite angles were noted to give rise to stronger Rh–B and Rh–H interactions, as evidenced by downfield ^{11}B NMR chemical shifts and upfield ^{1}H NMR chemical shifts. Notably, a σ-borane complex did not form for x = 2 (i.e. $Ph_2PCH_2CH_2PPh_2$), which demonstrates the tipping point where η^6-binding of the FC_6H_5 solvent outcompetes η^2-H_3B•NMe_3 coordination. These weak rhodium-borane interactions were found to be advantageous in catalysis, with small bite angles promoting faster dehydrocoupling of H_3B•NMe_2H to form $[H_2BNMe_2]_2$, e.g. TOFs from 180 h^{-1} (x = 5) to 1250 h^{-1} (x = 3).[7] For x = 2 no dehydrocoupling was observed, likely due to preferential binding of FC_6H_5 over σ-complexation of the amine–borane. Demonstration of this comes from comparison of the binding mode of the *B*-phenyl-substituted amine–borane H_2PhB•NMe_3 with {$Rh(PR_3)_2$}$^+$ fragments: wide bite angles favour amine–borane σ-coordination, tighter ones arene coordination, e.g. [Rh($PiPr_3$)$_2$(η^2-(BH)-H_2PhB•NMe_3)][BAr^F_4], [P–Rh–P =

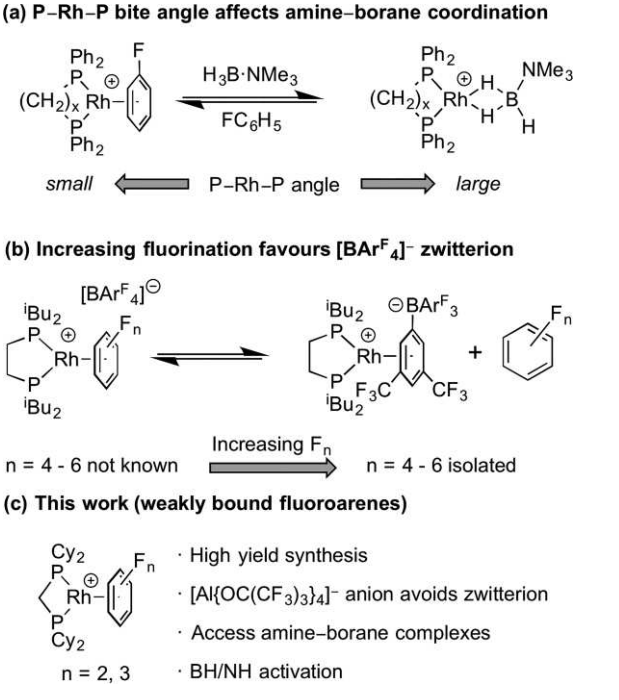

Scheme 1. (a) Displacement of FC_6H_5 by H_3B•NMe_3 (x = 3–5). [BAr^F_4]$^-$ anion not shown.[7] (b) Zwitterion formation from fluoroarene complexes.[11] (c) Preparation of fluoroarene complexes in this work. [Al{OC(CF_3)$_3$}$_4$]$^-$ anion not shown.

[a] *Department of Chemistry, Chemistry Research Laboratory, University of Oxford, Mansfield Road, Oxford OX1 3TA, UK*
E-mail: andrew.weller@chem.ox.ac.uk
http://research.chem.ox.ac.uk/andrew-weller.aspx
[b] *Institute of Chemical Sciences, Heriot Watt University, Edinburgh EH14 4AS, UK*
E-mail: S.A.Macgregor@hw.ac.uk
http://cic.eps.hw.ac.uk/

Supporting information and ORCID(s) from the author(s) for this article are available on the WWW under https://doi.org/10.1002/ejic.201700600.

101.86(3)°], and [Rh{*i*Pr$_2$P(CH$_2$)$_3$P*i*Pr$_2$}(η^6-H$_2$PhB•NMe$_3$)][BAr$^F_4$] [P–Rh–P = 94.04(4)°].[10]

Empirically the P–Rh–P bite angle has an inverse effect on arene binding in [Rh(bisphosphine)(arene)]$^+$ cations, with η^6-arene binding more favourable for smaller bite angle ligands,[7,12,13] for which we also suggest amine–borane σ-complexation is weaker. One way to mitigate these competing effects is to use more weakly binding arene ligands. η^6-Fluoroarenes are increasingly popular as weakly binding ligands that offer an operationally unsaturated metal centre.[14] However, the vast majority of cases are limited to FC$_6$H$_5$ examples, with a few examples of F$_2$C$_6$H$_4$ ligation,[7,14–17] due to the generally weaker binding of arenes with increasing degrees of fluorination.[18,19] Recently, the binding strength of fluoroarenes has been assessed using the [Rh(*i*Bu$_2$PCH$_2$CH$_2$P*i*Bu$_2$)(η^6-F$_n$C$_6$H$_{6-n}$)][BAr$^F_4$] scaffold. These studies showed that complexes could be accessed in situ for *n* = 0–3 (Scheme 1b),[11] whereas for more highly fluorinated analogues (*n* = 4–6) the reduced coordinating ability of the arene means that π complexation of the [BAr$^F_4$]$^-$ counterion becomes more favourable, and the zwitterionic complex [Rh(*i*Bu$_2$PCH$_2$CH$_2$P*i*Bu$_2$){η^6-(3,5-(CF$_3$)$_2$C$_6$H$_3$)BAr$^F_3$}] was observed as the sole product. Similar π-coordination of [BAr$^F_4$]$^-$ is now well established.[16,20–23]

With these observations in hand, we speculated that in order to synthesise an amine–borane complex with small bite angle bisphosphine supporting co-ligand a very weakly ligating fluoroarene would be needed to be coupled with manipulation of the anion to avoid zwitterion formation. In this contribution we demonstrate that Rh-complexes with the exceptionally small bite angle Cy$_2$PCH$_2$PCy$_2$ (dcpm) ligand[13,24] combined with moderately fluorinated arenes can be accessed using the [Al{OC(CF$_3$)$_3$}$_4$]$^-$ anion, thus providing a route to synthetically useful quantities of a trifluorobenzene complex (Scheme 1c). From such complexes flows the coordination chemistry of amine–boranes, and subsequent BH/NH activation, that results in a new dehydrocoupling route to bridging borylene complexes.

Results and Discussion

To avoid competition from zwitterion formation through coordination of [BAr$^F_4$]$^-$, the very weakly coordinating anion [Al{OC(CF$_3$)$_3$}$_4$]$^-$ was employed, the use of which has been pioneered and widely applied by Krossing.[25,26] Hydrogenation of [Rh(dcpm)(COD)][Al{OC(CF$_3$)$_3$}$_4$] (COD = cyclooctadiene) in 1,2-F$_2$C$_6$H$_4$ or 1,2,3-F$_3$C$_6$H$_3$ solution gave the corresponding fluoroarene complexes [Rh(dcpm)(F$_n$C$_6$H$_{6-n}$)][Al{OC(CF$_3$)$_3$}$_4$] [*n* = 2 (**1**), 3 (**2**)], Scheme 2. Trace quantities of other, more strongly coordinating, arenes in the commercially available solvents lead to impurities of the form [Rh(dcpm)(arene)][Al{OC(CF$_3$)$_3$}$_4$].[27] In the case of **1** these are minimal (<10 %), but for **2** considerable quantities are observed. This can be simply overcome by performing the synthesis of **2** in concentrated solution (0.17 M, 100 mg in 0.4 cm^3), thereby decreasing the ratio of [impurities]:[Rh] such that **2** is formed in >95 % spectroscopic yield. Both complexes **1** and **2** can be isolated as analytically pure yellow crystals in 78 % and 82 % yields respectively after crystallisation by addition of pentane. For comparison, the analogous [BAr$^F_4$]$^-$ complexes [Rh(dcpm)(F$_n$C$_6$H$_{6-n}$)][BAr$^F_4$] (*n* = 2, 3) were similarly prepared. Both species were observed in situ, and [Rh(dcpm)(1,2-F$_2$C$_6$H$_4$)][BAr$^F_4$] (**3**) could be isolated in 82 % yield as the only product. However, [Rh(dcpm)(1,2,3-F$_3$C$_6$H$_3$)][BAr$^F_4$] (**4**) forms the zwitterion complex [Rh(dcpm){η^6-(3,5-(CF$_3$)$_2$C$_6$H$_3$)-BAr$^F_3$}], (**5**), upon standing (Scheme 2). For [Rh(dcpm)(1,2-F$_2$C$_6$H$_4$)][BAr$^F_4$] slower partial conversion to **5** occurs over days,[28] and a single crystal X-ray structural determination confirmed its formulation (Scheme 2). To avoid such complications all future work was conducted exclusively with the [Al{OC(CF$_3$)$_3$}$_4$]$^-$ anion.

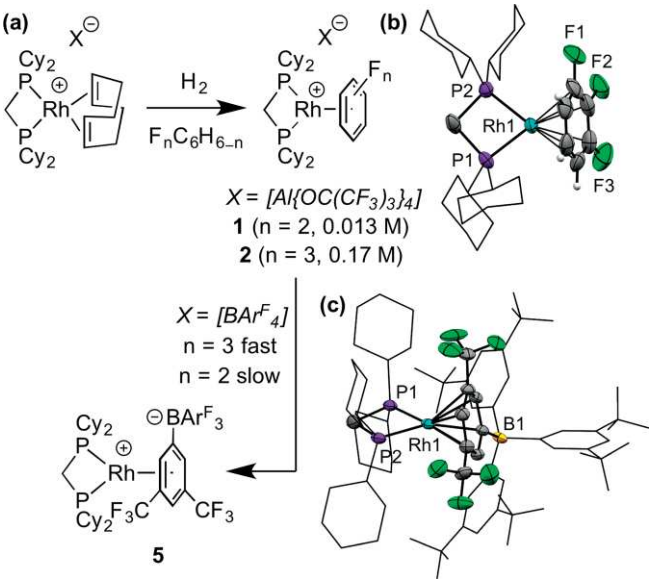

Scheme 2. (a) Preparation of η^6-fluoroarene complexes [Rh(dcpm)(η^6-F$_n$C$_6$H$_{6-n}$)][X] {X = [Al{OC(CF$_3$)$_3$}$_4$]: *n* = 2 (**1**), 3 (**2**); X = [BAr$^F_4$]: *n* = 2 (**3**), 3 (**4**)} and η^6-zwitterion [Rh(dcpm){η^6-(3,5-(CF$_3$)$_2$C$_6$H$_3$)BAr$^F_3$}] (**5**). (b) Solid-state structure of the cationic portion of complex **2**, alkyl hydrogen atoms omitted. Major disorder component shown only. Displacement ellipsoids are shown at the 50 % probability level. Selected bond lengths [Å] and angles [°]: Rh–C$_{aryl}$ range: 2.346(5)–2.263(5); Rh1–P1, 2.2452(10); Rh1–P2, 2.2397(10); P1–Rh1–P2, 73.06(4). (c) Solid-state structure of **5**, hydrogen atoms omitted, [BAr$^F_4$] simplified. Displacement ellipsoids are shown at the 50 % probability level. Selected bond lengths [Å] and angles [°]: Rh–C$_{aryl}$ range 2.425(6)–2.274(6); Rh1–P1, 2.2512(17); Rh1–P2, 2.2478(16); P1–Rh1–P2, 72.44(6).

In the ^{31}P{^{1}H} NMR spectra of **1** and **2** downfield shifts and increased Rh–P couplings relative to the precursor complexes are observed (**1**: δ –10.4, *J*(RhP) 168 Hz; **2**: δ –10.9, *J*(RhP) 167 Hz; cf. [Rh(dcpm)(COD)][Al{OC(CF$_3$)$_3$}$_4$]: δ –27.4, *J*(RhP) 126 Hz). In the ^{19}F{^{1}H} NMR spectrum the fluoroarene resonances shift downfield upon complexation, with those of **2** observed at δ –146.7 (2 F) and –167.1 (1 F), relative to free 1,2,3-F$_3$C$_6$H$_3$ (δ –136.8, –163.5), as described previously for related systems.[29–31]

Characterisation of **1** and **2** included a single-crystal X-ray crystallographic study (Scheme 2b for **2**, supporting materials for **1**), and complex **2** is the first structurally characterised example of an F$_3$C$_6$H$_3$-transition metal complex. Significant disorder of the fluoroarene ring between different rotomers means that discussion of the geometric parameters is not appropriate, but the structure does demonstrate arene binding and the

acute nature of the P–Rh–P angle [73.06(4)°]. The only previously reported example of 1,2,3-$F_3C_6H_3$ binding to a transition metal is [Rh(*i*$Bu_2PCH_2CH_2P$*i*Bu_2)(η^6-1,2,3-$F_3C_6H_3$)][BAr^F_4], the characterisation of which was limited to in situ NMR spectroscopy and mass spectrometry as it is formed in equilibrium with its [BAr^F_4]$^-$ coordinated zwitterion.[11] Here, for **2**, the combination of synthesis using concentrated solutions to overcome trace impurities and employing the very weakly coordinating anion [Al{$OC(CF_3)_3$}$_4$]$^-$ to obviate zwitterion formation allows for reliable access to such highly fluorinated arene complexes.

After establishing an effective route to weakly bound fluoroarene species **1** and **2** their reactivity with amine–boranes was investigated. Starting with $H_3B{\cdot}NMe_3$, which has no N–H groups and thus does not undergo dehydrocoupling, treatment of **1** with one equivalent of $H_3B{\cdot}NMe_3$ in 1,2-$F_2C_6H_4$ solution gave a mixture of **1** and the target complex [Rh(dcpm)(η^2-$H_3B{\cdot}NMe_3$)][Al{$OC(CF_3)_3$}$_4$] (**6**) in a ratio of 9:1 (as measured by $^{31}P\{^1H\}$ NMR spectroscopy). Addition of a second equivalent of $H_3B{\cdot}NMe_3$ decreased this ratio to 4:1, demonstrating that 1,2-$F_2C_6H_4$ binding is competitive with that of $H_3B{\cdot}NMe_3$. In contrast, for the more weakly bound 1,2,3-$F_3C_6H_3$ complex (**2**) reaction with $H_3B{\cdot}NMe_3$ in 1,2,3-$F_3C_6H_3$ solvent afforded **6** as the major product (81 % by $^{31}P\{^1H\}$ NMR spectroscopy), Scheme 3, alongside a collection of uncharacterised [Rh(dcpm)(arene)][Al{$OC(CF_3)_3$}$_4$] species (13 %) and other minor impurities. Moving to more concentrated solutions [0.17 M] did not significantly increase the yield of **6**, and clearly these minor impurities bind slightly more strongly than the amine–borane.

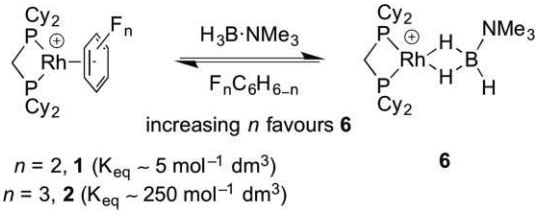

Scheme 3. Formation of [Rh(dcpm)(η^2-$H_3B{\cdot}NMe_3$)][Al{$OC(CF_3)_3$}$_4$] (**6**) (n = 2, 3). [Al{$OC(CF_3)_3$}$_4$]$^-$ anion not shown.

The NMR spectra of **6** resemble those of the analogous [Rh{$Ph_2P(CH_2)_nPPh_2$}(η^2-$H_3B{\cdot}NMe_3$)][BAr^F_4] complexes (n = 3–5).[7] In the $^{31}P\{^1H\}$ NMR spectrum of **6** a doublet is observed at δ –3.7 [J(RhP) 145 Hz]. The ^{11}B NMR spectrum contains a broad resonance at δ = 16.3; and the corresponding σ-bound Rh···H–B resonances appear at δ –1.75 as a very broad singlet (integral 3 H) in the ^1H NMR spectrum indicating rapid exchange between bridging and terminal B–H. Unfortunately, **6** did not survive ESI-MS conditions, and attempts to crystallise **6** resulted in decomposition, an indication of its relative instability.

Having access to small bite angle bisphosphine complexes that were capable of binding amine–boranes, albeit made in situ, their ability to dehydrocouple $H_3B{\cdot}NMe_2H$ was evaluated, as we have previously shown that the P–Rh–P bite angle has an influence on the rate of this process.[7] The dehydrocoupling of $H_3B{\cdot}NMe_2H$ in 1,2,3-$F_3C_6H_3$ solvent was investigated using 5 mol-% **2** (Scheme 4). The dehydrocoupling proved to be slow with only 14 % $H_3B{\cdot}NMe_2H$ consumption over 21 h to provide the dimeric aminoborane $[H_2BNMe_2]_2$ (8 %), alongside small quantities of other common dehydrocoupling products including transient $H_2B{=}NMe_2$, $H_3BNMe_2BH_2NMe_2H$, $[BH_2(NMe_2H)_2]^+$ and $H_2B(\mu\text{-}H)NMe_2BH_2$ as measured by ^{11}B NMR spectroscopy.[15,32–34] In the $^{31}P\{^1H\}$ NMR spectrum only one major phosphorus-containing species was observed (**7**), as a complex second-order multiplet at δ = 55.9, hinting at the formation of a dimeric species.[35] A very broad resonance is observed in the ^{11}B NMR spectrum at δ = 59.0, with nothing observed to lower field. In the ^1H NMR spectrum two very well resolved multiplets were observed in the high field region at δ = –4.87 and –7.91, with relative integrals of 2:1 respectively, which do not sharpen upon ^{11}B decoupling, but do simplify on decoupling ^{31}P. This suggests there are no significant ^{11}B···^1H interactions. In the ESI–MS spectrum, a peak at m/z = 1080.51 is observed, with an isotope pattern consistent with the gross formulation of a bimetallic monocation [{Rh(dcpm)}$_2H_3$($BNMe_2$)]$^+$. A similar dimerisation has been seen upon reaction of [Rh{$R_2P(CH_2)_3PR_2$}(η^6-FC_6H_5)][BAr^F_4] (R = *i*Pr, Ph) with $H_3B{\cdot}NH_3$, where the bridging aminoborane [{Rh($R_2P(CH_2)_3PR_2$)}$_2$(μ-H)(μ-H_2BNH_2)][BAr^F_4] [R = *i*Pr (**I**), Ph (**II**)] is formed, and the data for **7** are similar.[36]

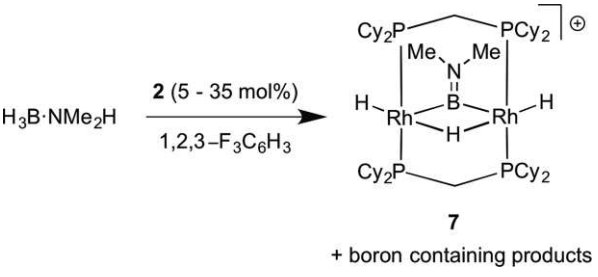

Scheme 4. Attempted dehydrocoupling of $H_3B{\cdot}NMe_2H$ and formation of [{RhH(μ-dcpm)}$_2$(μ-H)(μ-$BNMe_2$)][Al{$OC(CF_3)_3$}$_4$] (**7**). [Al{$OC(CF_3)_3$}$_4$]$^-$ anion not shown.

Crystalline material of complex **7** was obtained by recrystallisation from 1,2,3-$F_3C_6H_3$/pentane. In the bulk this was always contaminated with a boron-containing species identified as the boronium salt $[H_2B(NMe_2H)_2]^+$ [$\delta(^{11}B)$ = –2.0 ppm, J(BH) = 115 Hz; lit. $\delta(^{11}B)$ = –2.8 ppm, J(BH) = 113 Hz],[32] but this did allow a single-crystal X-ray diffraction study to be performed, the results of which are shown in Figure 1. The solid-state structure shows a rearrangement of the bisphosphine ligands upon dimerisation, and complex **7** contains bridging dcpm ligand in an A-frame motif[37] and an aminoborylene $BNMe_2$ group. The {Rh(μ-dcpm)}$_2$ construct resembles that of other binuclear rhodium systems with similar ligands.[38,39] Although the hydride ligands were not located in the final Fourier difference map, the combination of NMR spectroscopic evidence and DFT studies (vide infra) confirm the presence of one bridging hydride *trans*-disposed to one terminal Rh–H at each Rh centre, with the overall formulation [{RhH(μ-dcpm)}$_2$(μ-H)(μ-$BNMe_2$)][Al{$OC(CF_3)_3$}$_4$] (**7**). The geometry about each Rh is *pseudo*-square pyramidal, interestingly with a vacant coordination site *trans* to the borylene ligand. The cation has overall non-crystallographic C_{2v} symmetry. The Rh–B distances [2.015(6) and 1.983(7) Å] are shorter than those in the related bridging aminoborylene complex [{Rh(η^5-C_5H_5)(CO)}$_2${μ-$BN(SiMe_3)_2$}] [2.054(2) Å][40] and aminoborane complex [{Rh(P*i*$Pr_2(CH_2)_3$-

P*i*Pr$_2$)}$_2$(μ-H)(μ-BH$_2$NH$_2$)][BAr$^F{}_4$] [**I**, 2.055(5), 2.070(5) Å][36] but fall within the range seen for monomeric rhodium aminoboryl complexes of 2.034–1.929 Å.[10,41,42] The B–N distance in **7** [1.379(8) Å] is comparable to that measured in bridging aminoborylenes, for example [{Rh(η^5-C$_5$H$_5$)(CO)}$_2${μ-BN(SiMe$_3$)$_2$}] [1.399(6) Å],[40] and the only structurally characterised μ-BNMe$_2$ example [{Mn(η^5-C$_5$H$_5$)(CO)$_2$}$_2$(μ-BNMe$_2$)] [1.39(1) Å].[43]

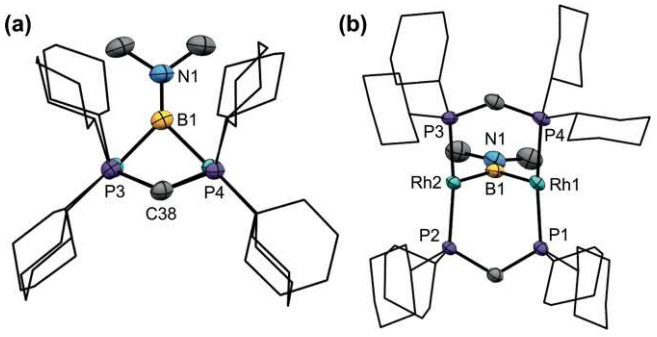

Figure 1. Solid-state structure of the cationic portion of complex **7**, hydrogen atoms omitted. (a) Viewed down the P–Rh–P axis. (b) Viewed down the B–N axis. Displacement ellipsoids are shown at the 50 % probability level. Selected distances [Å] and angles [°]: Rh1···Rh2, 2.8266(5); Rh1–B1, 2.015(6); Rh2–B1, 1.983(7); B1–N1 1.379(8); Rh1–P1, 2.2931(13); Rh1–P4, 2.3084(13); Rh2–P2, 2.2983(13); Rh2–P3, 2.2953(13); P1–Rh1–P4, 172.66(5); P2–Rh2–P3, 172.81(5).

The ^{11}B NMR chemical shift observed for **7** (δ = 59.0) suggests a bridging amino*borane* motif [cf. **I**, δ(^{11}B) 51.1].[36] However, the sharp signals observed for the hydrides in the ^{1}H NMR spectrum, that are unaffected by ^{11}B coupling, point to a bridging dihydrido amino*borylene* motif, which would be expected to show lower field chemical shifts in the ^{11}B NMR spectra (>90 ppm),[40,44] although examples have been observed as far upfield as 74 ppm.[45] An obvious geometric distinction between a bridging aminoborane (μ-H$_2$BNR$_2$) and a bridging aminoborylene dihydride (μ-BNR$_2$) structure is the orientation of the NR$_2$ moiety with respect to the RhBRh plane, as depicted in Figure 2. In the former case, e.g. **I**, a significant twist angle of 30.92° is observed between the RhBRh and HNH planes of **I** so as to maximise the orbital overlap between the B–H bonds

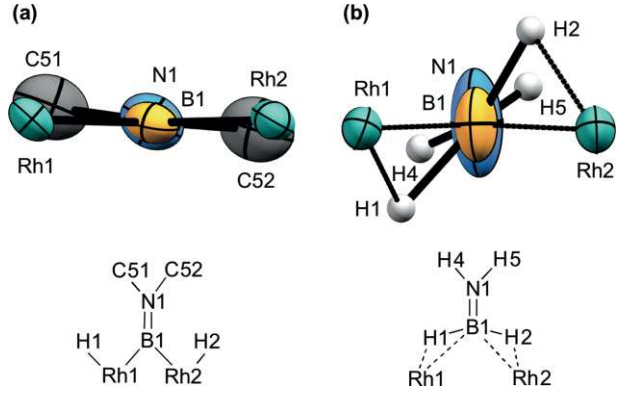

Figure 2. Solid state structures of the Rh$_2$BNR$_2$ cores of (a) μ-aminoborylene **7** (R = Me), and (b) μ-aminoborane **I** (R = H)[36] viewed down the B–N axis. Displacement ellipsoids are shown at the 50 % probability level. Twist angles [°]: (a) plane(Rh1B1Rh2)/plane(C51N1C52) 7.25°; (b) plane(Rh1B1Rh2)/plane(H4N1H5) 30.92°.

and Rh centres.[36] This interaction is not present in **7** or [{Mn(η^5-C$_5$H$_5$)(CO)$_2$}$_2$(μ-BNMe$_2$)],[43] hence minimal twist angles are observed between the RhBRh and CNC planes of 7.25° and 8.38°, respectively. We postulate that the vacant coordination site *trans* to boron in complex **7** modifies the chemical shift to such an extent that the signal for the borylene is observed about 30 ppm to higher field than expected.

Density functional theory calculations[46] in conjunction with Quantum Theory of Atoms in Molecules (QTAIM) and Natural Bond Orbital (NBO) analyses have been employed to investigate the electronic structure of **7** (see Figure 3). Full geometry optimisation with the BP86 functional provided excellent agreement for the heavy atom positions and confirmed the presence of two terminal and one bridging hydride and square-pyramidal coordination around each Rh centre. Long H1···B1 and H2···B1 distances in excess of 2.9 Å preclude any direct bonding interaction and this is confirmed by the lack of a bond path between these centres (Figure 3a). In contrast, bond paths are computed between B1 and both Rh centres, as well as between Rh1/H1

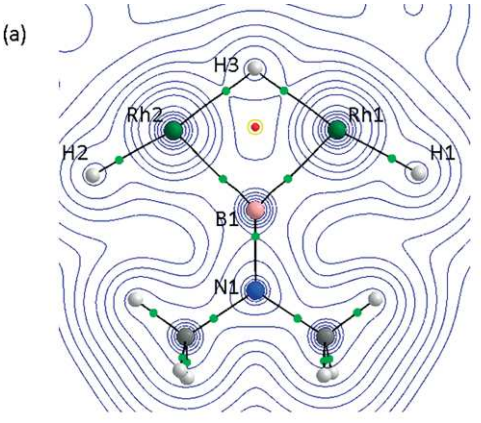

(b)

	Distance/Å	$\rho(r)$	ε	$H(r)$
Rh1–B1	2.01	0.12	0.05	-0.08
Rh1–H1	1.61	0.13	0.01	-0.06
Rh1–H3	1.80	0.08	0.02	-0.02
B1–N1	1.41	0.20	0.13	-0.16

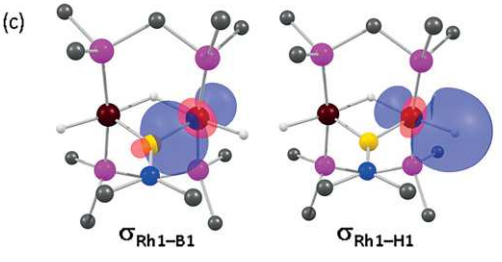

Figure 3. (a) Contour plot of the total electron density of the central part of **7** presented in the {Rh1B1Rh2} plane highlighting key bond paths and associated bond critical points (BCP, in green) and the ring critical point (RCP, in red). (b) Computed key distances and BCP metrics (a.u) for bond paths associated with Rh1 [$\varrho(r)$ = electron density; ε = bond ellipticity, $H(r)$ = total energy density; the computed structure has effective C$_{2v}$ symmetry and so equivalent data are associated with Rh2, see Supporting Information]. (c) Natural bond orbitals highlighting Rh1–B1 and Rh1–H1 bonding (C–H hydrogens removed and Cy groups truncated at C1 for clarity).

and Rh2/H2. The associated bond critical points (BCPs) exhibit negative values of the total energy density *H(r)* and low ellipticities, ε, characteristics of σ-bonding that is predominantly covalent in nature. This contrasts with the μ-H_2BNH_2 motif in **I** where the BCPs associated with the Rh–H and Rh–B bond paths have large ellipticities of about 0.5 au reflecting the anisotropic *B*-agostic Rh←H–B interaction.[36] The presence of the bridging hydride in **7** means that a ring critical point is seen between the Rh centres. The computed Rh1•••Rh2 distance of 2.85 Å is in good agreement with the experimental value of 2.8266(5) Å. The lack of any Rh1•••Rh2 interaction is confirmed in the NBO analysis which highlights three Rh-based (d-orbital) lone pairs, as well as Rh1–H1/Rh2–H2 and Rh1–B1/Rh2–B1 bonding orbitals. In contrast NBO calculations on [{Rh(η^5-C_5H_5)(CO)}$_2${μ-BN($SiMe_3$)$_2$}] clearly locate a Rh–Rh bonding orbital consistent with the presence of a metal–metal bond (see Supporting Information).

The formation of **7** is postulated to proceed in a similar manner to **I** and **II** (Scheme 5).[36] Displacement of the fluoroarene ligand enables initial formation of a σ-H_3B•NMe_2H complex (**A**), analogous to complex **6**. Subsequent B–H oxidative cleavage yields the intermediate aminoboryl **B**, from which elimination of the boronium salt $[H_2B(NMe_2H)_2]^+$ (observed at the end of the reaction) generates a neutral "{RhH(dcpm)}" fragment **C**. NMe_2H arises from H_3B•NMe_2H dissociation, consistent with the observation of H_2B(μ-H)NMe_2BH_2 in the reaction. It has previously been shown that hydrogenation of [Rh($R_2PCH_2PR_2$)(η^3-CH_2Ph)] (R = Cy, *i*Pr) affords the A-frame bridging bisphosphine complex [RhH(μ-$R_2PCH_2PR_2$)(μ-H)]$_2$,[47] and an equivalent rearrangement has been noted in the reaction of [Rh(*i*Pr_2PCH_2P*i*Pr_2)(CO)(η^3-C_3H_5)] with H_2 to form [Rh(μ-*i*Pr_2-PCH_2P*i*Pr_2)(CO)(μ-H)]$_2$.[39] Presumably these dimerisations are driven by ring strain. We thus propose that dimerisation of **C** first forms a neutral bridging A-frame complex, [RhH(dcpm)]$_2$ which then undergoes protonation by a half equivalent of $[H_2B(NMe_2H)_2]^+$ to form a bridging aminoborane **D**. Complex **7** then results from a double B–H activation of **D** to form a bridging aminoborylene dihydride. Interestingly this does not occur with the $R_2P(CH_2)_3PR_2$ ligands in **I** and **II** in which there is not an A-frame motif.[36] Similar geminal C–H activations of alkenes are effected by [{Ir(μ-$Et_2PCH_2PEt_2$)(CO)}$_2$(μ-H)(μ-CO)]$^+$[38] and [{Ir(μ-$Ph_2PCH_2PPh_2$)}$_2$(μ-CO)(CH_3)(CO)]$^+$.[48,49] Such C–H activations are proposed to proceed via a cooperative mechanism wherein π-complexation of H_2C=CRR′ to one metal enables σ-CH complexation at the other metal and consequently C–H cleavage. This bears parallels with the double B–H activation of transient H_2B=NMe_2 observed here, although aminoboranes bind end-on rather than the side-on mode adopted by alkenes.[50,51] Aminoborane to aminoborylene transformations by double B–H activation of H_2B=NR_2 (R = Cy, *i*Pr) have been observed with mononuclear iridium and ruthenium complexes,[52,53] and related transformations on boranes are also known.[54,55] However, to the best of our knowledge the complete amine–borane to aminoborylene transformation is unprecedented, and represents a new method for the preparation of bridging borylenes.

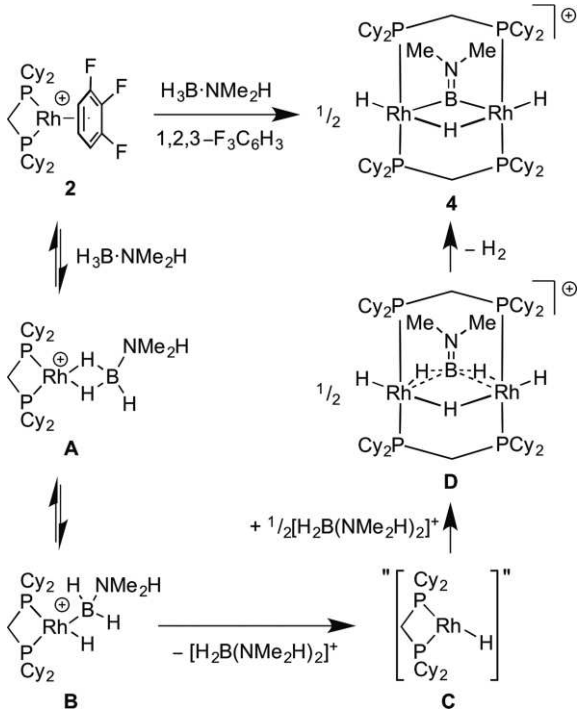

Scheme 5. Proposed mechanism of formation of **7**. [Al{$OC(CF_3)_3$}$_4$]$^-$ anion not shown.

Conclusions

The marriage of the very weakly coordinating anion [Al{$OC(CF_3)_3$}$_4$]$^-$ and fluoroarenes 1,2-$F_2C_6H_4$ and 1,2,3-$F_3C_6H_3$ enables the synthesis and isolation of a previously inaccessible σ-amine–borane complex of a small bite angle phosphine. The ring strain imposed by the dcpm ligand leads to unprecedented chemistry with amine–boranes, culminating in formation of a bimetallic aminoborylene [{RhH(μ-dcpm)}$_2$(μ-H)(μ-$BNMe_2$)]-[Al{$OC(CF_3)_3$}$_4$], the nature of which is confirmed by DFT calculations and QTAIM and NBO analyses.

Experimental Section

All manipulations, unless otherwise stated, were performed under an argon atmosphere using standard Schlenk line and glovebox techniques. Glassware was oven dried at 130 °C overnight and flame dried under vacuum prior to use. Pentane and CH_2Cl_2 were dried using a Grubbs type solvent purification system (MBraun SPS-800) and degassed by three successive freeze-pump-thaw cycles. 1,2-$F_2C_6H_4$ (purchased from Fluorochem, pretreated with alumina), 1,2,3-$F_3C_6H_3$ (purchased from Fluorochem, pretreated with alumina) and CD_2Cl_2 were dried with CaH_2, vacuum distilled and stored over 3 Å molecular sieves. H_3B•NMe_3 and H_3B•NMe_2H were purchased from Sigma–Aldrich and sublimed prior to use. Li[Al{$OC(CF_3)_3$}$_4$][25] and [Rh(COD)Cl]$_2$[56] were prepared by literature methods. All other chemicals were obtained from commercial sources and used as received.

NMR spectra were recorded with a Bruker AVIIIHD 500 or Bruker AVIIIHD 400 nanobay spectrometer at room temperature, unless otherwise stated. In 1,2-$F_2C_6H_4$ and 1,2,3-$F_3C_6H_3$, ^{1}H NMR spectra were prelocked to a sample of C_6D_6 (25 %) and 1,2-$F_2C_6H_4$ (75 %)

and referenced to the centre of the downfield solvent multiplet, δ = 7.07 and 6.96 ppm, respectively. ^{31}P, ^{11}B and ^{19}F NMR spectra were referenced against 85 % H_3PO_4 (external), $BF_3{\cdot}OEt_2$ (external) and CCl_3F (external), respectively. Chemical shifts (δ) are quoted in ppm and coupling constants (J) in Hz. ESI-MS data were recorded with a Bruker MicrOTOF instrument interfaced with a glove-box. Microanalyses were performed by Stephen Boyer at London Metropolitan University.

$[Rh(COD)_2][Al\{OC(CF_3)_3\}_4]$: Prepared according to the literature procedure for $[Rh(COD)_2][BAr^F{}_4]$.[57] An orange solution of $[Rh(COD)Cl]_2$ (0.585 g, 1.19 mmol) and 1,5-cyclooctadiene (0.2 mL) in CH_2Cl_2 (20 mL) was degassed by bubbling argon through the solution for 15 min. The solution was then added dropwise to a colourless slurry of $Li[Al\{OC(CF_3)_3\}_4]$ (2.31 g, 2.37 mmol) in CH_2Cl_2 (60 mL) with vigorous stirring at ambient temperature. The colour of the slurry immediately changed to dark red. The reaction mixture was stirred at ambient temperature for a further 16 h and then filtered. The supernatant was then concentrated under vacuum (ca. 50 mL). Cooling to –20 °C overnight afforded a red crystalline solid which was isolated by decanting, washed with pentane (2 × 2 mL) and dried under vacuum. Further concentration followed by cooling afforded a second crop. Yield (2.53 g, 83 %). ^{1}H NMR (CD_2Cl_2, 400 MHz): δ = 5.26 (s, 8 H, COD-CH), 2.55 (s, 16 H, COD-CH_2) ppm. $^{19}F\{^1H\}$ NMR (CD_2Cl_2, 376 MHz): δ = –75.8 (s) ppm. ESI-MS (1,2-$F_2C_6H_4$, 60 °C, 4.5 kV): *m/z* 319.10 (calculated 319.09 for $[Rh(COD)_2]^+$ fragment). $C_{32}H_{24}AlF_{36}O_4Rh$ (1286.35): calcd. C 29.88, H 1.88; found C 29.93, H 1.91.

$[Rh(dcpm)(COD)][Al\{OC(CF_3)_3\}_4]$: Prepared according to the literature procedure for $[Rh(dcpe)(COD)][BAr^F{}_4]$.[58] A solution of $[Rh(COD)_2][Al\{OC(CF_3)_3\}_4]$ (400.2 mg, 0.3111 mmol) in CH_2Cl_2 (10 mL) was treated dropwise with a solution of dcpm (127.1 mg, 0.3111 mmol) in CH_2Cl_2 (70 mL) at –78 °C with vigorous stirring. Upon complete addition the colour of the reaction mixture changed from burgundy to orange. The reaction mixture was warmed to ambient temperature and stirred for 16 h. The solution was concentrated to 10 mL under vacuum and pentane (50 mL) was added to precipitate an orange solid which was isolated by filtration, washed with pentane (3 × 10 mL) and dried under vacuum. Yield 436.9 mg (0.2753 mmol, 89 %). The powder was then extracted into the minimum amount of CH_2Cl_2 and layered with pentane, which afforded large orange crystals suitable for an X-ray diffraction study. ^{1}H NMR (500 MHz, CD_2Cl_2, 298 K): δ = 5.38 (br. s, 4 H, COD-CH), 3.00 (td, $^2J_{PH}$ = 10, $^3J_{RhH}$ = 1 Hz, 2 H, PCH_2P), 2.33 (s, 8 H, COD-CH_2), 2.11–1.77 (br. m, 24 H, Cy), 1.45–1.22 (br. m, 20 H, Cy) ppm. $^{31}P\{^1H\}$ NMR (202 MHz, CD_2Cl_2, 298 K): δ = –27.4 (d, $^1J_{RhP}$ = 126 Hz) ppm. $^{19}F\{^1H\}$ NMR (470 MHz, CD_2Cl_2, 298 K): δ = –75.8 (s) ppm. ESI-MS (1,2-$F_2C_6H_4$, 60 °C, 4.5 kV): *m/z* 619.32 (calculated 619.31 for $[Rh(dcpm)(COD)]^+$ fragment). $C_{49}H_{58}AlF_{36}O_4P_2Rh$ (1586.76): calcd. C 37.09, H 3.68; found C 37.18, H 3.59.

$[Rh(dcpm)(COD)][BAr^F{}_4]$: Prepared according to the literature procedure for $[Rh(dcpe)(COD)][BAr^F{}_4]$.[58] A solution of $[Rh(COD)_2][BAr^F{}_4]$ (349 mg, 0.295 mmol) in CH_2Cl_2 (40 mL) was treated dropwise with a solution of dcpm (122 mg, 0.299 mmol) in CH_2Cl_2 (20 mL) at –78 °C with vigorous stirring. Upon complete addition the colour of the reaction mixture changed from burgundy to orange. The reaction mixture was warmed to ambient temperature and stirred for 16 h. The solution was concentrated to 5 mL under vacuum and pentane (50 mL) was added to precipitate an orange solid which was isolated by filtration, washed with pentane (3 × 10 mL) and dried under vacuum. Yield 408 mg (0.275 mmol, 93 %). The powder was then extracted into the minimum amount of CH_2Cl_2 and layered with pentane, which afforded large orange crystals suitable for an X-ray diffraction study. ^{1}H NMR (500 MHz, CD_2Cl_2, 298 K): δ = 7.72 (s, 8 H, *ortho*-$BAr^F{}_4$), 7.56 (s, 4 H, *para*-$BAr^F{}_4$), 5.37 (br. s, 4 H, COD-CH), 2.99 (t, br, $^2J_{PH}$ = 10 Hz, 2 H, PCH_2P), 2.31 (s, 8 H, COD-CH_2), 2.08–1.76 (br. m, 24 H, Cy), 1.43–1.20 (br. m, 20 H, Cy) ppm. $^{31}P\{^1H\}$ NMR (202 MHz, CD_2Cl_2, 298 K): δ = –27.5 (d, $^1J_{RhP}$ = 126 Hz) ppm. $^{19}F\{^1H\}$ NMR (470 MHz, CD_2Cl_2, 298 K): δ = –62.9 (s) ppm. ESI-MS (1,2-$F_2C_6H_4$, 60 °C, 4.5 kV): *m/z* 619.32 (calculated 619.31 for $[Rh(dcpm)(COD)]^+$ fragment). $C_{65}H_{70}BF_{24}P_2Rh$ (1482.88): calcd. C 52.65, H 4.76; found C 52.41, H 4.81.

$[Rh(dcpm)(1,2\text{-}F_2C_6H_4)][Al\{OC(CF_3)_3\}_4]$ (1): $[Rh(dcpm)(COD)][Al\{OC(CF_3)_3\}_4]$ (100 mg, 63.0 µmol) was dissolved in 1,2-$F_2C_6H_4$ (5 mL) in a J. Young flask. The solution was freeze-pump-thaw degassed three times and refilled with H_2 (4 atm). The reaction mixture was stirred for 16 h, over which time the colour the solution changed from orange to yellow. Volatiles and excess H_2 were removed under vacuum and the resultant solid was washed with pentane (2 × 5 mL). The solid was extracted into the minimum volume of CH_2Cl_2, filtered and layered with pentane to afford yellow crystals suitable for X-ray diffraction which were isolated by filtration and dried under vacuum. Yield: 80 mg (49 µmol, 78 %). ^{1}H NMR (400 MHz, CD_2Cl_2, 298 K): δ = 6.90 (m, 2 H, $F_2C_6H_4$), 6.17 (m, 2 H, $F_2C_6H_4$), 2.70 (td, $^2J_{PH}$ = 10, $^3J_{RhH}$ = 2 Hz, 2 H, PCH_2P), 1.94–1.63 (br. m, 24 H, Cy), 1.40–1.03 (br. m, 20 H, Cy) ppm. $^{31}P\{^1H\}$ NMR (162 MHz, CD_2Cl_2, 298 K): δ = –10.4 (d, $^1J_{RhP}$ = 168 Hz) ppm. $^{19}F\{^1H\}$ NMR (376 MHz, CD_2Cl_2, 298 K): δ = –75.8 (s, 36 F, CF_3), –146.3 (d, $^2J_{RhF}$ = 3 Hz, 2 F, $F_2C_6H_4$) ppm. ESI-MS (1,2-$F_2C_6H_4$, 60 °C, 4.5 kV): *m/z* 625.24 (calculated 625.24 for $[Rh(dcpm)(1,2\text{-}F_2C_6H_4)]^+$ fragment). $C_{47}H_{50}AlF_{38}O_4P_2Rh$ (1592.67): calcd. C 35.44, H 3.16; found C 35.51, H 3.19.

$[Rh(dcpm)(1,2,3\text{-}F_3C_6H_3)][Al\{OC(CF_3)_3\}_4]$ (2): $[Rh(dcpm)(COD)][Al\{OC(CF_3)_3\}_4]$ (107 mg, 67.4 µmol) was dissolved in 1,2,3-$F_3C_6H_3$ (0.4 mL) in a high pressure J. Young NMR tube. The solution was freeze-pump-thaw degassed three times and refilled with H_2 (4 atm). The solution was stirred for 4 h, over which time the solution changed from orange to yellow. Excess H_2 was removed by three freeze-pump-thaw cycles and the fluoroarene complex was characterised by NMR spectroscopy in situ. The solution was filtered and layered with pentane to afford yellow crystals suitable for X-ray diffraction which were isolated by filtration and dried under vacuum. Yield: 88 mg (55 µmol, 82 %). ^{1}H NMR (400 MHz, 1,2,3-$F_3C_6H_3$, 298 K): δ = 6.56 (br. s, 2 H, 1,3-$F_3C_6H_3$), 6.49 (br. m, 1 H, 2-$F_3C_6H_3$), 2.85 (t, br, $^2J_{PH}$ = 10 Hz, 2 H, PCH_2P), 2.00–1.67 (br. m, 24 H, Cy), 1.44–1.13 (br. m, 20 H, Cy and cyclooctane) ppm. $^{31}P\{^1H\}$ NMR (162 MHz, 1,2,3-$F_3C_6H_3$, 298 K): δ = –10.9 (d, $^1J_{RhP}$ = 167 Hz) ppm. $^{19}F\{^1H\}$ NMR (376 MHz, 1,2,3-$F_3C_6H_3$, 298 K): δ = –75.8 (s, 36 F, CF_3), –146.7 (br. d, $^3J_{FF}$ = 30 Hz, 2 F, 1,3-$F_3C_6H_3$), –167.1 (br. d, $^3J_{FF}$ = 30, $^2J_{RhF}$ = 5 Hz, 1 F, 2-$F_3C_6H_3$) ppm, $[Rh(dcpm)(1,2,3\text{-}F_3C_6H_3)][Al\{OC(CF_3)_3\}_4]$ did not persist under ESI-MS conditions. $C_{47}H_{49}AlF_{39}O_4P_2Rh$ (1610.66): calcd. C 35.05, H 3.07; found C 35.19, H 3.01.

$[Rh(dcpm)(1,2\text{-}F_2C_6H_4)][BAr^F{}_4]$ (3): $[Rh(dcpm)(COD)][BAr^F{}_4]$ (50 mg, 33.7 µmol) was dissolved in 1,2-$F_2C_6H_4$ (5 mL) in a J. Young flask. The solution was freeze-pump-thaw degassed three times and refilled with H_2 (4 atm). The reaction mixture was stirred for 16 h, over which time the colour the solution changed from orange to yellow. Volatiles and excess H_2 were removed under vacuum and the resultant solid was washed with pentane (2 × 2 mL) and dried under vacuum. Crystals of **3** were obtained by layering a 1,2-$F_2C_6H_4$ solution of **3** with pentane. Yield: 41 mg (27.5 µmol, 82 %). ^{1}H NMR (400 MHz, CD_2Cl_2, 298 K): δ = 7.74 (s, 8 H, *ortho*-$BAr^F{}_4$), 7.58 (s, 4 H, *para*-$BAr^F{}_4$), 6.91 (m, 2 H, $F_2C_6H_4$), 6.15 (m, 2 H, $F_2C_6H_4$), 2.70 (td, $^2J_{PH}$ = 10, $^3J_{RhH}$ = 2 Hz, 2 H, PCH_2P), 1.94–1.63 (br. m, 24

H, Cy), 1.39–1.03 (br. m, 20 H, Cy) ppm. $^{31}P\{^{1}H\}$ NMR (162 MHz, CD_2Cl_2, 298 K): δ = –10.3 (d, $^{1}J_{RhP}$ = 169 Hz) ppm. $^{19}F\{^{1}H\}$ NMR (376 MHz, CD_2Cl_2, 298 K): δ = –62.9 (s, 36 F, BAr^F_4), –146.2 (br. s, 2 F, $F_2C_6H_4$) ppm. ESI-MS (1,2-$F_2C_6H_4$, 60 °C, 4.5 kV): *m/z* 625.24 (calculated 625.24 for $[Rh(dcpm)(1,2\text{-}F_2C_6H_4)]^+$ fragment). $C_{63}H_{62}BF_{26}P_2Rh$ (1488.79): calcd. C 50.82, H 4.20; found C 50.93, H 4.26.

In-situ Preparation of [Rh(dcpm)(1,2,3-$F_3C_6H_3$)][BAr^F_4] (4) and Isolation of [Rh(dcpm){η⁶-(3,5-$(CF_3)_2C_6H_3$)BAr^F_3}] (5): [Rh(dcpm)(COD)][BAr^F_4] (54 mg, 36.4 μmol) was dissolved in 1,2,3-$F_3C_6H_3$ (0.4 mL) in a high pressure J. Young NMR tube. The solution was freeze-pump-thaw degassed three times and refilled with H_2 (4 atm). The solution was stirred for 4 h, over which time the solution changed from orange to yellow. Excess H_2 was removed by three freeze-pump-thaw cycles and the fluoroarene complex was characterised by NMR spectroscopy in situ. ^{1}H NMR (500 MHz, 1,2,3-$F_3C_6H_3$, 298 K): δ = 8.06 (s, 8 H, *ortho*-BAr^F_4), 7.48 (s, 4 H, *para*-BAr^F_4), 6.57 (br. s, 2 H, 1,3-$F_3C_6H_3$), 6.50 (br. m, 1 H, 2-$F_3C_6H_3$), 2.87 (t, br, $^{2}J_{PH}$ = 10 Hz, 2 H, PCH_2P), 2.02–1.70 (br. m, 24 H, Cy), 1.41–1.20 (br. m, 20 H, Cy and cyclooctane) ppm. $^{31}P\{^{1}H\}$ NMR (202 MHz, 1,2,3-$F_3C_6H_3$, 298 K): δ = –10.9 (d, $^{1}J_{RhP}$ = 168 Hz) ppm. $^{19}F\{^{1}H\}$ NMR (470 MHz, 1,2,3-$F_3C_6H_3$, 298 K): δ = –63.5 (s, 24 F, CF_3), –146.0 (br. d, $^{3}J_{FF}$ = 30 Hz, 2 F, 1,3-$F_3C_6H_3$), –166.0 (t, br, $^{3}J_{FF}$ = 30 Hz, 1 F, 2-$F_3C_6H_3$) ppm. Attempts to crystallise [Rh(dcpm)(1,2,3-$F_3C_6H_3$)][BAr^F_4] by layering with pentane afforded a yellow solution of [Rh(dcpm){η⁶-(3,5-$(CF_3)_2C_6H_3$)BAr^F_3}]. The solvent was removed under vacuum and the residue was extracted into pentane. Slow cooling of the pentane solution to –20 °C afforded crystals of [Rh(dcpm){η⁶-(3,5-$(CF_3)_2C_6H_3$)BAr^F_3}] (22 mg, 16 μmol, 44 %). ^{1}H NMR (400 MHz, F_6C_6, 298 K): δ = 7.58 (s, 6 H, *ortho*-BAr^F_4 non-coordinated rings), 7.40 (s, 3 H, *para*-BAr^F_4 non-coordinated rings), 7.21 (s, 2 H, *ortho*-BAr^F_4 Rh-coordinated ring), 6.95 (s, 1 H, *para*-BAr^F_4 Rh-coordinated ring), 2.80 (br. s, 2 H, PCH_2P), 2.04–1.67 (br. m, 24 H, Cy), 1.36–1.12 (br. m, 20 H, Cy) ppm. $^{31}P\{^{1}H\}$ NMR (162 MHz, F_6C_6, 298 K): δ = –12.7 (d, $^{1}J_{RhP}$ = 172 Hz) ppm. $^{19}F\{^{1}H\}$ NMR (376 MHz, F_6C_6, 298 K): δ = –61.5 (s, 1 F, BAr^F_4 Rh-coordinated ring), –64.1 (s, 3 F, BAr^F_4 non-coordinated rings) ppm. $C_{57}H_{58}BF_{24}P_2Rh$ (1374.70): calcd. C 49.80, H 4.25; found C 49.89, H 4.34.

[Rh(dcpm)($H_3B{\cdot}NMe_3$)][Al{$OC(CF_3)_3$}$_4$] (6): [Rh(dcpm)(1,2,3-$F_3C_6H_3$)][Al{$OC(CF_3)_3$}$_4$] (30.0 mg, 18.6 μmol) and $H_3B{\cdot}NMe_3$ (2.8 mg, 38 μmol) were dissolved in 1,2,3-$F_3C_6H_3$ (0.3 mL) and stirred for 1 min. The solution turned red, and pentane (ca 3 mL) was added to give a red oil, which, upon sonicating, afforded a red oily solid. This was isolated by filtration, washed with pentane (3 × 3 mL) and dried under vacuum. Attempts to purify **6** resulted in isolation of an oily red solid, NMR spectroscopy of which showed no improvement in purity (ca. 80 % pure). Yield 16 mg (10 μmol, 55 %). NMR spectra were collected immediately upon dissolution in CD_2Cl_2 as extended time in solution leads to decomposition of **3**. ^{1}H NMR (400 MHz, CD_2Cl_2, 298 K): δ = 2.91 (br. s, 2 H, PCH_2P), 2.79 (s, 9 H, NMe_3), 2.04–1.75 (br. m, 24 H, Cy), 1.46–1.23 (br. m, 20 H, Cy), –1.75 (s, v br, 3 H, BH_3, sharpens upon ^{1}H-decoupling) ppm. ^{11}B (128 MHz, CD_2Cl_2, 298 K): δ = 16.3 (s, br) ppm. $^{11}B\{^{1}H\}$ (128 MHz, CD_2Cl_2, 298 K): δ = 16.1 (s, br) ppm. $^{31}P\{^{1}H\}$ (162 MHz, CD_2Cl_2, 298 K): δ –3.4 (d, $^{1}J_{RhP}$ = 145 Hz) ppm. [Rh(dcpm)($H_3B{\cdot}NMe_3$)][Al{$OC(CF_3)_3$}$_4$] did not persist under ESI-MS conditions. Satisfactory elemental analysis was not obtained.

[{RhH(μ-dcpm)}$_2$(μ-H)(μ-$BNMe_2$)][Al{$OC(CF_3)_3$}$_4$] (7): [Rh(dcpm)(1,2,3-$F_3C_6H_3$)][Al{$OC(CF_3)_3$}$_4$] (81.0 mg, 50.3 μmol) and $H_3B{\cdot}NMe_2H$ (9.3 mg, 16 μmol) were dissolved in 1,2,3-$F_3C_6H_3$ (0.4 mL) and stirred for two days. Pentane (5 mL) was added to form a yellow precipitate which was isolated by filtration and washed with pentane (3 × 3 mL). Recrystallisation from 1,2,3-$F_3C_6H_3$/pentane afforded **7** as yellow crystals suitable for X-ray diffraction (23 mg) that were contaminated with recalcitrant $[H_2B(NMe_2H)_2][Al\{OC(CF_3)_3\}_4]$. ^{1}H NMR (500 MHz, 1,2,3-$F_3C_6H_3$, 298 K): δ = 2.78 (s, 6 H, NMe_2), 2.21 (t, $^{2}J_{PH}$ = 5 Hz, 2 H, PCH_2P), 2.18 (t, $^{2}J_{PH}$ = 5 Hz, 2 H, PCH_2P), 2.66–1.24 (m, 88 H, Cy), –4.87 (br. m, 2 H, Rh-H), –7.91 (br. m, 1 H, RhHRh) ppm. ^{11}B (160 MHz, 1,2,3-$F_3C_6H_3$, 298 K): δ = 59.0 (s, v br) ppm. $^{11}B\{^{1}H\}$ (160 MHz, 1,2,3-$F_3C_6H_3$, 298 K): δ = 59.0 (s, v br) ppm. $^{31}P\{^{1}H\}$ NMR (202 MHz, 1,2,3-$F_3C_6H_3$, 298 K): δ = 55.9 (m) ppm. ESI-MS (1,2-$F_2C_6H_4$, 60 °C, 4.5 kV): *m/z* 1080.51 (calculated 1080.51 for $[\{RhH(\mu\text{-}dcpm)\}_2(\mu\text{-}H)(\mu\text{-}BNMe_2)]^+$ fragment). Satisfactory elemental analysis results could not be obtained due to contamination of bulk samples with $[H_2B(NMe_2H)_2][Al\{OC(CF_3)_3\}_4]$.

Acknowledgments

The Engineering and Physical Sciences Research Council (EPSRC) (A. S. W. and S. A. M., EP/M024210/1; N. A. B., DTP Studentship).

Keywords: Amines · Rhodium · Boranes · Fluoroarenes · Phosphines

[1] H. C. Johnson, T. N. Hooper, A. S. Weller, *Top. Organomet. Chem.* **2015**, *49*, 153–220.
[2] E. M. Leitao, T. Jurca, I. Manners, *Nat. Chem.* **2013**, *5*, 817–829.
[3] A. Rossin, M. Peruzzini, *Chem. Rev.* **2016**, *116*, 8848–8872.
[4] M. Shimoi, S. Nagai, M. Ichikawa, Y. Kawano, K. Katoh, M. Uruichi, H. Ogino, *J. Am. Chem. Soc.* **1999**, *121*, 11704–11712.
[5] Y. Kawano, M. Hashiva, M. Shimoi, *Organometallics* **2006**, *25*, 4420–4426.
[6] A. E. W. Ledger, C. E. Ellul, M. F. Mahon, J. M. J. Williams, M. K. Whittlesey, *Chem. Eur. J.* **2011**, *17*, 8704–8713.
[7] R. Dallanegra, A. P. M. Robertson, A. B. Chaplin, I. Manners, A. S. Weller, *Chem. Commun.* **2011**, *47*, 3763–3765.
[8] P. Dierkes, P. W. N. M. van Leeuwen, *J. Chem. Soc., Dalton Trans.* **1999**, 1519–1529.
[9] A. B. Chaplin, A. S. Weller, *Inorg. Chem.* **2010**, *49*, 1111–1121.
[10] A. Kumar, I. K. Priest, T. N. Hooper, A. S. Weller, *Dalton Trans.* **2016**, *45*, 6183–6195.
[11] S. D. Pike, I. Pernik, R. Theron, J. S. Mcindoe, A. S. Weller, *J. Organomet. Chem.* **2015**, *784*, 75–83.
[12] S. D. Pike, T. Kramer, N. H. Rees, S. A. Macgregor, A. S. Weller, *Organometallics* **2015**, *34*, 1487–1497.
[13] I. Pernik, J. F. Hooper, A. B. Chaplin, A. S. Weller, M. C. Willis, *ACS Catal.* **2012**, *2*, 2779–2786.
[14] S. D. Pike, M. R. Crimmin, A. B. Chaplin, *Chem. Commun.* **2017**, *53*, 3615–3633.
[15] T. M. Douglas, A. B. Chaplin, A. S. Weller, X. Yang, M. B. Hall, *J. Am. Chem. Soc.* **2009**, *131*, 15440–15456.
[16] S. D. Pike, A. L. Thompson, A. G. Algarra, D. C. Apperley, S. A. Macgregor, A. S. Weller, *Science* **2012**, *337*, 1648–1651.
[17] K. Bambridge, R. M. G. Roberts, *J. Organomet. Chem.* **1991**, *401*, 125–132.
[18] J. I. Wu, F. G. Pühlhofer, P. von Ragué Schleyer, R. Puchta, B. Kiran, M. Mauksch, N. J. R. van Eikema Hommes, I. Alkorta, J. Elguero, *J. Phys. Chem. A* **2009**, *113*, 6789–6794.
[19] S. Kawahara, S. Tsuzuki, T. Uchimaru, *Chem. Eur. J.* **2005**, *11*, 4458–4464.
[20] A. R. O'Connor, P. S. White, M. Brookhart, *Organometallics* **2010**, *29*, 5382–5389.
[21] J. Powell, A. Lough, T. Saeed, *J. Chem. Soc., Dalton Trans.* **1997**, 4137–4138.
[22] A. R. O'Connor, M. Brookhart, *J. Polym. Sci., Part A Polym. Chem.* **2010**, *48*, 1901–1912.
[23] T. M. Douglas, E. Molinos, S. K. Brayshaw, A. S. Weller, *Organometallics* **2007**, *26*, 463–465.
[24] F. Eisenträger, A. Göthlich, I. Gruber, H. Heiss, C. A. Kiener, C. Krüger, J. U. Notheis, F. Rominger, G. Scherhag, M. Schultz, B. F. Straub, M. A. O. Vollan, P. Hofmann, *New J. Chem.* **2003**, *27*, 540–550.

[25] I. Krossing, *Chem. Eur. J.* **2001**, *7*, 490–502.
[26] I. Krossing, I. Raabe, *Angew. Chem. Int. Ed.* **2004**, *43*, 2066–2090; *Angew. Chem.* **2004**, *116*, 2116.
[27] 1,2,3-$F_3C_6H_3$ was purchased from Fluorochem, treated with alumina, dried with CaH_2 and vacuum distilled before use. GC–MS analysis of the purified solvent identified the arenes FC_6H_5, $F_2C_6H_4$, $FCl_2C_6H_3$, $F_2ClC_6H_3$, $F_2Cl_2C_6H_2$, $F_3ClC_6H_2$ and $F_3BrC_6H_2$ as trace impurities.
[28] This reactivity profile suggests a dissociative process for substitution.
[29] V. S. Khandkarova, S. P. Gubin, B. A. Kvasov, *J. Organomet. Chem.* **1970**, *23*, 509–515.
[30] H. Ssekaalo, J. J. Lagowski, C. M. Seymour, *Inorg. Chim. Acta* **1991**, *183*, 91–95.
[31] M. J. McGlinchey, T.-S. Tan, *Can. J. Chem.* **1974**, *52*, 2439–2443.
[32] M. Roselló-Merino, J. López-Serrano, S. Conejero, *J. Am. Chem. Soc.* **2013**, *135*, 10910–10913.
[33] C. A. Jaska, K. Temple, A. J. Lough, I. Manners, *J. Am. Chem. Soc.* **2003**, *125*, 9424–9434.
[34] C. J. Stevens, R. Dallanegra, A. B. Chaplin, A. S. Weller, S. A. Macgregor, B. Ward, D. McKay, G. Alcaraz, S. Sabo-Etienne, *Chem. Eur. J.* **2011**, *17*, 3011–3020.
[35] A. Rifat, N. J. Patmore, M. F. Mahon, A. S. Weller, *Organometallics* **2002**, *21*, 2856–2865.
[36] A. Kumar, N. A. Beattie, S. D. Pike, S. A. Macgregor, A. S. Weller, *Angew. Chem. Int. Ed.* **2016**, *55*, 6651–6656; *Angew. Chem.* **2016**, *128*, 6763.
[37] C. P. Kubiak, R. Eisenberg, *J. Am. Chem. Soc.* **1977**, *99*, 6129–6131.
[38] M. E. Slaney, D. J. Anderson, M. J. Ferguson, R. McDonald, M. Cowie, *Organometallics* **2012**, *31*, 2286–2301.
[39] H. Werner, M. Manger, M. Laubender, M. Teichert, D. Stalke, *J. Organomet. Chem.* **1998**, *569*, 189–194.
[40] H. Braunschweig, M. Forster, T. Kupfer, F. Seeler, *Angew. Chem. Int. Ed.* **2008**, *47*, 5981–5983; *Angew. Chem.* **2008**, *120*, 6070.
[41] C. Y. Tang, N. Phillips, J. I. Bates, A. L. Thompson, M. J. Gutmann, S. Aldridge, *Chem. Commun.* **2012**, *48*, 8096–8098.
[42] H. C. Johnson, E. M. Leitao, G. R. Whittell, I. Manners, G. C. Lloyd-Jones, A. S. Weller, *J. Am. Chem. Soc.* **2014**, *136*, 9078–9093.
[43] H. Braunschweig, T. Wagner, *Angew. Chem. Int. Ed. Engl.* **1995**, *34*, 825–826; *Angew. Chem.* **1995**, *107*, 904.
[44] H. Braunschweig, R. D. Dewhurst, V. H. Gessner, *Chem. Soc. Rev.* **2013**, *42*, 3197–3208.
[45] H. Braunschweig, M. Forster, K. Radacki, *Angew. Chem. Int. Ed.* **2006**, *45*, 2132–2134; *Angew. Chem.* **2006**, *118*, 2187.
[46] See Supporting Information for full details and references.
[47] M. D. Fryzuk, D. H. McConville, S. J. Rettig, *J. Organomet. Chem.* **1993**, *445*, 245–256.
[48] J. Dusan Ristic-Petrovic, D. Anderson, J. R. Torkelson, M. J. Ferguson, R. McDonald, M. Cowie, *Organometallics* **2005**, *24*, 3711–3724.
[49] D. Ristic-Petrovic, J. R. Torkelson, R. W. Hilts, R. McDonald, M. Cowie, *Organometallics* **2000**, *19*, 4432–4434.
[50] C. Y. Tang, A. L. Thompson, S. Aldridge, *Angew. Chem. Int. Ed.* **2010**, *49*, 921–925; *Angew. Chem.* **2010**, *122*, 933.
[51] C. Y. Tang, A. L. Thompson, S. Aldridge, *J. Am. Chem. Soc.* **2010**, *132*, 10578–10591.
[52] D. A. Addy, J. I. Bates, M. J. Kelly, I. M. Riddlestone, S. Aldridge, *Organometallics* **2013**, *32*, 1583–1586.
[53] M. O'Neill, D. A. Addy, I. Riddlestone, M. Kelly, N. Phillips, S. Aldridge, *J. Am. Chem. Soc.* **2011**, *133*, 11500–11503.
[54] G. Alcaraz, U. Helmstedt, E. Clot, L. Vendier, S. Sabo-Etienne, *J. Am. Chem. Soc.* **2008**, *130*, 12878–12879.
[55] N. Arnold, H. Braunschweig, R. D. Dewhurst, W. C. Ewing, *J. Am. Chem. Soc.* **2016**, *138*, 76–79.
[56] B. Guzel, M. A. Omary, J. P. Fackler Jr., A. Akgerman, *Inorg. Chim. Acta* **2001**, *325*, 45–50.
[57] G. Giordano, R. H. Crabtree, *Inorg. Synth.* **1979**, *19*, 218–220.
[58] S. D. Pike, F. M. Chadwick, N. H. Rees, M. P. Scott, A. S. Weller, T. Krämer, S. A. Macgregor, *J. Am. Chem. Soc.* **2015**, *137*, 820–833.

Received: May 21, 2017